THE IMPACT OF THE NUMBER OF ACTIVE CASTING STRANDS IN A THREE-STRAND TUNDISH ON TRANSITION AREAS

Peter ŠMIGURA, Branislav BUĽKO, Dominik DUBEC, Peter DEMETER, Jaroslav DEMETER, Lukáš FOGARAŠ, Slavomír HUBATKA, Andrii PYLYPENKO

Institute of Metallurgical Technologies and Digital Transformation, Faculty of materials, Metallurgy and Recycling Department of Metallurgy, Technical University of Košice, Košice, Slovakia, EU,
peter.smigura@student.tuke.sk

https://doi.org/10.37904/metal.2025.5106

Abstract

The presented research is focused on identifying differences in the lengths of transition areas during the continuous casting of steel in a three-strand "T"-type tundish, considering various numbers of active strands. The study compares results from three types of measurements: in the first measurement, casting was simulated with three active strands (full capacity); in the second measurement, the simulation was realised with the middle strand disabled; and in the third measurement, the continuous casting process was simulated with one of the outer strands disabled. The measurement results indicate which mode, involving one inactive strand, is more suitable when one strand needs to be disabled in real-world operations during continuous steel casting. The research was realised in the SimConT laboratory located at the Technical University of Košice, at the IMTECH Institute. The SimConT laboratory specializes in the physical modelling of continuous steel casting processes. For the measurements, a three-strand "T"-type tundish model was used, scaled at 1:3 relative to the actual tundish used in continuous steel casting operations at Železiarne Podbrezová a.s

Keywords: Steel, Continuous Casting Machine, Tundish, Intermix, Physical Modelling, F-Curve

1. INTRODUCTION

In the process of continuous steel casting on a continuous casting machine (CCM), the ideal condition occurs when casting is realised with the maximum number of active strands. However, this ideal state is influenced by several factors. Although infrequently, situations arise in steel plant operations where one casting strand is inactive and does not participate in the continuous casting process. The shutdown of a casting strand may be initiated either by the CCM operators or by the CCM control system. The CCM operator may deactivate one casting strand for various reasons. These reasons may include failures in upstream steel production units, such as the primary melting unit or secondary metallurgical treatment. These are situations where the upstream production stages are unable to deliver liquid steel to the CCM on time. In such cases, one casting strand may be disabled to slow down the casting process on the CCM and prevent a complete interruption of continuous casting on all strands [1].

Other operator-initiated reasons for deactivating a casting strand include damage to the submerged entry nozzle, steel overflow, or recurring casting defects (e.g., surface cracks, incorrect dimensions, or shape). A casting strand can also be shut down by the CCM control system itself. This occurs when the system evaluates that it is unsafe to continue the continuous casting process on the respective strand. This may be due to the exceeding of set limits, such as pressure and water flow rates for primary and secondary cooling, roll pressure in the straightening segment, or the frequency of mold oscillation [1,2]. During continuous casting of liquid steel on the CCM with one inactive strand, it is often necessary to continue the casting process. When liquid steel from two main ladles—i.e., from two heats—is mixed in the tundish, transition areas are formed [3,4]. These transition areas arise during the ladle changeover on the rotary ladle turret. After the first main ladle is emptied, a second full main ladle with liquid steel is placed above the tundish. A remaining amount of liquid steel from the first ladle stays in the tundish to ensure the continuity of the casting process. Steel from the second main ladle is then poured into the tundish, which still contains liquid steel from the previous ladle. During the homogenization of liquid steel in the tundish, steel from both main ladles is mixed, resulting in the formation of transition areas. These transition areas contain liquid steel originating from both main ladles. Directly during the continuous casting of steel, determining the length and location of transition areas is very complex. Therefore, research on transition areas is conducted using physical models. These models are constructed either to scale or in full size, based on real equipment. Physical models are used to study processes that are either unfeasible or only partially feasible under actual continuous casting conditions [1]. At the IMTECH Institute, in the SimConT laboratory, three physical models are available: a 1:1 scale model of the mold, a 1:3 scale model of a two-strand tundish, and a 1:3 scale model of a three-strand tundish relative to the actual equipment [2].

2. METHODOLOGY

The presented research consisted of three measurements. In the first measurement, the tundish model was simulated with all three casting strands active. In the second measurement, only the outer strands No. 1 and No. 3 were active, while the middle strand No. 2 was inactive. In the third measurement, one of the outer strands No. 3 was inactive, while the outer strand No. 1 and the middle strand No. 2 were active. All three measurements were carried out using a 1:2 scale model of a three-strand tundish relative to the actual equipment. Each measurement lasted 10 minutes, i.e., 600 seconds. During each second, 10 values of electrical conductivity in siemens [S] were recorded for each strand. This means that 6000 values were recorded for each strand during each measurement. All three measurements were realized under standard operational flow rates for all measured strands (3 × 8 l/min). This means that the outlet nodes were not obstructed—in real conditions, this corresponds to a submerged entry nozzle with no clogged ports, and the overall outlet from the tundish was free of blockages. The internal configuration of the tundish model remained unchanged, so identical conditions were ensured for all three measurements. **Figure 1** shows the model of the three-strand tundish with the layout of individual casting strands [2].

Figure 1 Three-stream tundish model with labelled pouring strands

In physical modelling of steel production processes, water is used as a substitute for liquid steel. Water at room temperature 20 °C and molten steel at the casting temperature of 1600 °C have relatively similar kinematic viscosity [1]. The kinematic viscosity of liquid steel at the casting temperature of 1600 °C is approximately 0.913×10^{-6} m²/s, while the kinematic viscosity of water at room temperature 20 °C is approximately 1×10^{-6} m²/s. At the outlets of the tundish model, probes are installed that measure electrical conductivity at the mentioned interval of 0.1 seconds. Utility water was filled into the tundish model. The water was filled to a level of 300 mm from the bottom of the tundish. The volume of water in the model was 0.182 m³. This volume corresponds to 10.1 tons of liquid steel under real conditions. Tracer substances $KMnO_4$ and KCl were added to the entire water volume in the model. Potassium permanganate $KMnO_4$ serves a visual purpose during the simulation. Potassium chloride KCl increases the conductivity of the utility water, and the changes in electrical conductivity between water with KCl and water without KCl are the primary focus of these measurements. The water, $KMnO_4$, and KCl were thoroughly mixed and homogenized throughout the entire volume of the tundish model. In the physical modelling of transition areas in the tundish, a key moment occurs when clean utility water begins to flow into the prepared solution of KCl and $KMnO_4$ (time t_0). In the real casting process, this moment corresponds to the opening of the second full main ladle. At this moment, all three measurements conducted in this research begin. After a sufficient evaluation period (10 minutes) had passed, the data on changes in conductivity were further processed. The data were evaluated on all active strands. The electrical conductivity values of pure water (without additives) were subtracted from the measured data. This adjustment is important to prevent the results from being distorted. The adjusted values were then normalized by dividing them by the highest measured value. Through this mathematical operation, the electrical conductivity was transformed into a dimensionless quantity ranging from 1 to 0 [5]. This adjustment of the measured data is essential for comparing results and determining the transition areas. The calculated dimensionless values were compared with the Pareto rules 80:20 and 90:10, which in the context of dimensionless values in the 0–1 range correspond to thresholds of 0.8:0.2 and 0.9:0.1. To evaluate the transition zone between successive melts, the commonly applied 80/20 and 90/10 criteria were used. These are based on the analysis of residence time distribution (RTD) curves obtained from physical or numerical simulations. The 80/20 criterion defines the transition period as the time interval during which the concentration of the new fluid at the outlet increases from 20 % to 80 %. The 90/10 criterion applies a stricter range, from 10 % to 90 %, and is often used when a more precise assessment of mixing behaviour is required. Both metrics are widely adopted in steelmaking research to quantify the effectiveness of flow control systems and the sharpness of the transition between different steel grades. When these Pareto thresholds were exceeded, time values were recorded. These time values were then converted using the factor 1.41423. This factor represents the ratio of physical phenomena in the actual equipment and in the model. The three-strand tundish model is scaled at 1:2, so it was necessary to calculate the time scaling factor between the real tundish and the model. This value was calculated using the formula:

$$M_\tau = M^{1/2} = 1/2^{1/2} = 0{,}7071 \qquad \frac{1}{0.7071} = 1.41423 \tag{1}$$

Where $M\tau$ is the time scale between the tundish model and the real tundish (i.e., the actual equipment), and M is the length scale ratio of the model to the real equipment. From this calculation, it can be concluded that the phenomena observed in the tundish model occur 1.41423 times faster than in the actual tundish.

After converting the time data from the tundish model to the actual equipment, the data were further converted to the mass of steel cast through each strand. For each strand, the casting rate was 5.283 kg/s. Following these adjustments, the mass of steel that flowed through each strand from the moment the second main ladle was opened was calculated, and the start and end points of the transition areas were defined under the specific conditions.

3. MEASUREMENTS AND RESULTS

SIMULATION WITH ALL THREE STRANDS ACTIVE

In this simulation, all three casting strands were active. **Figure 2** shows the results already converted to dimensionless values over time. Time $\mathbf{t_0}$ represents the opening of the second main ladle.

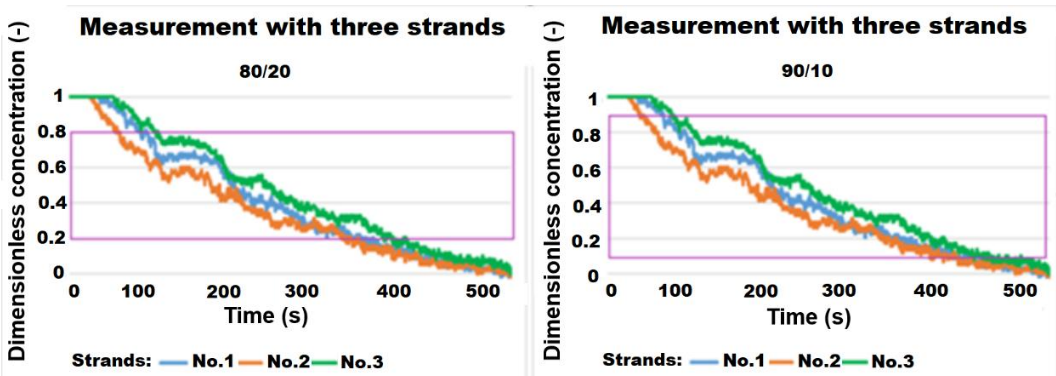

Figure 2 Simulation Results for Three Casting Strands

The graphs in **Figure 3** show the points where the f-curves, derived from the measured values, intersect the thresholds defined by the respective rules. When comparing the results across individual strands, a difference can be observed between casting strand No. 2 and the outer casting strands. As shown in **Figure 1**, this casting strand is located near the openings in the baffle, which divides the tundish into two parts—the inflow section from the main ladle and the working section [6,7,8]. As a result, liquid steel from the second main ladle reaches casting strand No. 2 earlier than it does the outer strands. **Table 1** show the data defining the boundaries of the transition areas according to the respective rules, measured from time t_0 in the actual equipment.

Table 1 Masses in the Actual Equipment According to the (left 80/20), (right 90/10) Rule in the Three-Strand Simulation

Mass in the Actual Equipment	80	20
Strand no. 1	721.8 kg	2940.2 kg
Strand no. 2	513.3 kg	2854.3 kg
Strand no. 3	895.9 kg	3251.1 kg

Mass in the Actual Equipment	90	10
Strand no. 1	562.6 kg	3514.1 kg
Strand no. 2	331.0 kg	3459.5 kg
Strand no. 3	645.6 kg	3688.2 kg

SIMULATION WITH INACTIVE MIDDLE CASTING STRAND NO. 2

In this simulation, the middle casting strand No. 2 was inactive. The active casting strands were the outer strands, labelled No. 1 and No. 3.

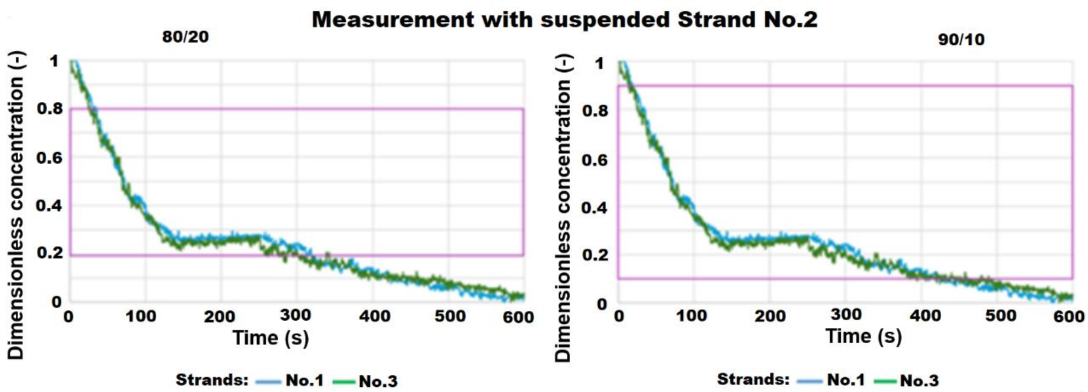

Figure 3 Simulation Results with Inactive Casting Strand No. 2

From the graphs in **Figure 3**, it can be observed that the resulting F-curves are similar on both outer casting strands. As shown in Figure 1, the three-strand tundish model can be divided into two mirror-symmetrical parts along the central axis [6]. The outer strands are equally distant from the centre of the tundish model, which results in similar F-curves [9]. This observation is also supported by the values in **Table 2** and **Table 3**, where only minimal differences can be seen between the corresponding boundary points when converted to the actual equipment.

Table 2 Masses in the Actual Equipment According to the 80/20 Rule in the Simulation with Inactive Strand No. 2

Mass in the Actual Equipment	80	20
Strand no. 1	210.71 kg	2379.08 kg
Strand no. 3	198.01 kg	2249.07 kg

Table 3 Masses in the Actual Equipment According to the 90/10 Rule in the Simulation with Inactive Strand No. 2

Mass in the Actual Equipment	90	10
Strand no. 1	135.24 kg	3223.42 kg
Strand no. 3	128.52 kg	3241.35 kg

SIMULATION WITH INACTIVE OUTER CASTING STRAND NO. 3

In this simulation, one of the outer casting strands was inactive. Since outer casting strands No. 1 and No. 3 are positioned symmetrically along the central axis of the tundish model, the measured values also apply to active strand No. 3 in the case where strand No. 1 is inactive. The simulation with inactive casting strand No. 2 also demonstrated that the results on the outer strands are identical.

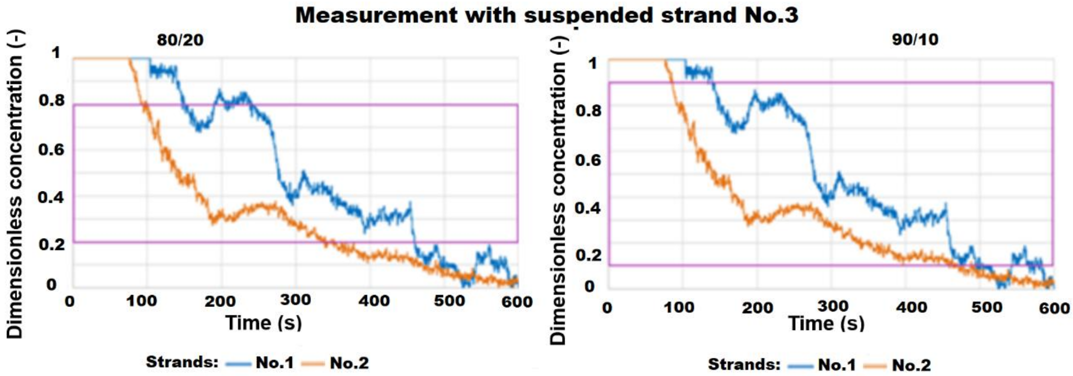

Figure 4 Simulation Results with Inactive Casting Strand No. 3

In the simulation with the inactive outer casting strand, the graphs in **Figure 4** show different behaviour of the F-curves on the middle and outer casting strands. On the middle casting strand No. 2, the transition area begins earlier, as this strand is located near the openings in the baffle of the tundish model. On the outer casting strand No. 1, the beginning of the transition area is recorded later. **Tables 4** and **Table 5** present the data according to the Pareto rules, converted directly to the actual equipment.

Table 4 Masses in the Actual Equipment According to the 80/20 Rule in the Simulation with Inactive Strand No. 3

Mass in the Actual Equipment	80	20
Strand no. 1	1781.32 kg	3434.13 kg
Strand no. 2	753.18 kg	2603.24 kg

Table 5 Masses in the Actual Equipment According to the 90/10 Rule in the Simulation with Inactive Strand No. 3

Mass in the Actual Equipment	90	10
Strand no. 1	1068.50 kg	4360.66 kg
Strand no. 2	644.83 kg	3517.82 kg

4. DISCUSSION

COMPARISON ON CASTING STRAND NO. 1

Table 6 Comparison of Results on Casting Strand No. 1 According to the 80/20 Rule

Strand no. 1 (80/20)	80	20
Simulation no. 1	721.8 kg	2940.2 kg
Simulation no. 2	210.71 kg	2379.08 kg
Simulation no. 3	1781.32 kg	3434.13 kg

Table 7 Comparison of Results on Casting Strand No. 1 According to the 90/10 Rule

Strand no. 1 (90/10)	90	10
Simulation no. 1	562.6 kg	3514.1 kg
Simulation no. 2	135.24 kg	3223.42 kg
Simulation no. 3	1068.50 kg	4360.66 kg

The results on casting strand No. 1 were first compared using the 80/20 rule, where the value 80 represents the start and 20 the end of the transition area **Table 6**. In the first simulation, the length of the transition area was 2218.4 kg. The first simulation represented the ideal state of continuous casting with all strands active. In the second simulation, with inactive middle strand No. 2, the transition area length was 2168.37 kg. When comparing the results of the first two simulations, it is evident that the lengths of the transition areas are comparable. In the third simulation, with an inactive outer casting strand, the transition area length was 1652.81 kg. According to the 80/20 rule, the transition area in the third simulation is the shortest.

Table 7 compares the results on casting strand No. 1 using the 90/10 rule. The value 90 defines the start of the transition area, and 10 defines the end. In the first simulation, the length of the transition area was 2951.5 kg. In the second simulation, this length was 3088.18 kg. Even according to the 90/10 rule, the lengths of the transition areas are comparable. In the third simulation, the length of the transition area was 3292.16 kg, making it the longest.

COMPARISON OF RESULTS ON STRAND NO. 2

Table 8 Comparison of Results on Casting Strand No. 2 According to the 80/20 Rule

Strand no. 2 (80/20)	80	20
Simulation no. 1	513.3 kg	2854.3 kg
Simulation no. 2	-	-
Simulation no. 3	753.18 kg	2603.24 kg

Table 9 Comparison of Results on Casting Strand No. 2 According to the 90/10 Rule

Strand no. 2 (90/10)	90	10
Simulation no. 1	331.0 kg	3459.5 kg
Simulation no. 2	-	-
Simulation no. 3	644.83 kg	3517.82 kg

Table 8 presents the simulation results on casting strand No. 2 according to the 80/20 rule. In the first simulation, the transition area had a length of 2341 kg. In the third simulation, the transition area length was 1850.06 kg. The results are comparable, including both the start and end points of the transition areas, as well as the overall length. In the second simulation, casting strand No. 2 was inactive. **Table 9** presents the simulation results according to the 90/10 rule on the middle casting strand No. 2. In the first simulation, the transition area length was 3128 kg, and in the third simulation, it was 2872.99 kg. Even according to the 90/10 rule, the length of the transition area is comparable, as are the start and end points of the compared transition areas.

CONCLUSION

The primary objective was to compare the simulation of the ideal casting process with all strands active (1st simulation) to the two simulations in which one specific casting strand was inactive. When comparing simulations 1 and 2, the results on the outer casting strands No. 1 and No. 3 were comparable. In the 2nd simulation, with the middle strand No. 2 inactive, the F-curves on the outer casting strands were relatively linear, and predicting the transition areas was straightforward. The results on the outer strands in the first two simulations were quite consistent.

With the middle casting strand inactive, the occurrence of stagnant flow zones in the tundish is likely, as indicated by the comparable results. In the 3rd simulation, with an inactive outer casting strand, correctly identifying the transition area on the active outer strand was more challenging. On the F-curve of the active outer casting strand, irregular increases in electrical conductivity were observed. Liquid steel from the first main ladle continued to penetrate the formed transition area. Especially under the 90/10 rule, determining the end of the transition area was difficult.

For this reason, based on the findings of this research, if one casting strand must be shut down, it is most effective to deactivate the middle strand. With casting strand No. 2 inactive, it is possible to clearly and symmetrically identify the transition areas on both outer casting strands.

ACKNOWLEDGEMENTS

This research was funded by project: Smart-Steel: AI-Driven control models for future steel production 09I05-03-V02-00016

REFERENCES

[1] MICHALEK, K., GRYC, K., SOCHA, L., TKADLECKOVÁ, M., SATERNUS, M., PIEPRZYCA, J., MERDER, T., PINDOR, L., Study of tundish slag entrainment using physical modelling. Archives of Metallurgy and Materials. 2016, vol. 61, pp. 257-260. DOI:10.1515/amm-2016-0048

[2] Laboratory of simulation of flow processes, Technical University of Košice, Institute of Metallurgy, Department of Metallurgy and Foundry. [Online]. 2017. [viewed: 2023-05-08]. Available from: https://ohaz.umet.fmmr.tuke.sk/lspp/index_en.html.

[3] CHATTERJEE, S., CHATOPPADHYAY, K., Transient steel quality under non-isothermal conditions in a multi-strand billet caster tundish: part II. Effect of a flow-control device. Ironmaking & Steelmaking, Minerals & Mining, 1. JULY 2017, DOI: 10.1080/03019233.2016.1214015

[4] FOGARAŠ L., BUĽKO B., DEMETER P., HUBATKA S., DEMETER J., ŠMIGURA P., Investigation of optimal transient conditions in t-shape tundish during steel intermixing. Metal 2023 Brno, Czech Republic, EU. May 17 - 19, 2023, 32nd International Conference on Metallurgy and Materials, pp. 52-58.

[5] HALL, Blair D., The Problem with'Dimensionless Quantities'. MODELSWARD. 2022. p. 116-125.

[6] MERDER, T., BOGUSŁAWSKI, A., JOWSA, J., The analysis of the conditions of steel flow in the tundish performed by a numerical method, Archives of Metallurgy and Materials. 2005, Vol 50, pp. 933-953.

[7] MERDER, T. Effect of casting flow rate on steel flow phenomena in tundish. Metalurgija. 2013, vol. 52, pp. 161-164.

[8] YADAV, J.N., SOMANI, S.K., PATIL, H.S. Investigation of fluid flow characterization in single strand tundish using flow developers and inclusions. AIP Conference Proceeding. 22. august 2024, p. 050002

[9] GRYC, K., MICHALEK, K., HUDZIECZEK, Z., TKADLEČKOVÁ, M. Physical modelling of flow pattern in 5-strand asymmetrical tundish with baffles. Conference proceedings METAL. 2010. p. 42-46.

[10] MICHALEK, K., GRYC K., SOCHA L., SATERNUS M., TKADLEČKOVÁ M., PIEPRZYCA J., MERDER T., PINDOR L. Study of tundish slag entrainment using physical modelling. Archives of Metallurgy and Materials, 2016, vol. 61, pp. 257-260.